Production of $\gamma\gamma$+2 jets from double parton scattering in proton-proton collisions at the LHC *

TAO Jun-Quan(陶军全)[1;1)] ZHANG Si-Jing(张思靓)[1,2] SHEN Yu-Qiao(沈玉乔)[1,2]
FAN Jia-Wei(范嘉伟)[1,2] CHEN Guo-Ming(陈国明)[1] CHEN He-Sheng(陈和生)[1]

[1] Institute of High Energy Physics, Chinese Academy of Sciences, Beijing 100049, China
[2] University of Chinese Academy of Sciences, Beijing 100049, China

Abstract: Cross sections for the production of pairs of photons plus two additional jets produced from double parton scattering in high-energy proton-proton collisions at the LHC are calculated for the first time. The estimates are based on the theoretical perturbative QCD predictions for the productions of $\gamma\gamma$ at next-to-next-to-leading-order, jet+jet and γ+jet at next-to-leading-order, for their corresponding single-scattering cross sections. The cross sections and expected event rates for $\gamma\gamma$+2 jets from double parton scattering, after typical acceptance and selections, are given for proton-proton collisions with the collision energy $\sqrt{s}$=13 TeV and integrated luminosity of 100 fb^{-1} planned for the following years, and also $\sqrt{s}$=14 TeV with 3000 fb^{-1} of integrated luminosity as the LHC design.

Key words: $\gamma\gamma$+2 jets production, double parton scattering, QCD

PACS: 11.80.La, 12.38.Bx, 25.20.Lj **DOI:** 10.1088/1674-1137/39/12/121001

1 Introduction

In proton-proton (pp) collisions with high energies at the Large Hadron Collider (LHC), particle production is dominated by multiple interactions of their constituent partons, with most particles from the hardest proton-proton scattering and the radiation and fragmentation of secondary partonic actions. The higher centre-of-mass energy leads to enhanced parton densities, which cause a sizable probability of two or more parton-parton scatterings within the same pp interaction [1, 2]. At LHC, various measurements of the differential distributions in W+jets [3, 4] and J/ψ+W [5] show that the excesses above the expectations from single parton scattering (SPS) are consistent with double parton scattering (DPS). Various measurements in other pp and p$\bar{\text{p}}$ collisions at $\sqrt{s}$=63 GeV [6], 630 GeV [7], and 1.8 TeV [8] are consistent with DPS contributions to multi-jet final states, as well as to γ+3-jet events at $\sqrt{s}$=1.8 TeV [9] and 1.96 TeV [10]. The measurements of DPS processes can provide valuable information on the transverse distribution of partons in the proton [11] and on the multi-parton correlations in the hadronic wave function [12]. DPS also constitutes the background for new physics searches at the LHC [13–15]. Additional searches for DPS have been proposed via double Drell-Yan, four jets and same-sign WW production [16–18].

In this paper, the cross section for the production of pairs of photons plus two additional jets produced from double parton scattering (DPS) in high-energy proton-proton collisions at the LHC are calculated for the first time. $\gamma\gamma$ final states have played a crucial role in the recent discovery of a new boson at the LHC [19, 20] and are also important in many new physics searches [21–24], in particular the search for extra spatial dimensions or cascade decays of heavy new particles. In particular, diphotons in combination with jets and missing energy occur in gauge-mediated SUSY scenarios. $\gamma\gamma$ or plus two additional jets also offers an important test of both perturbative and non-perturbative quantum chromodynamics (QCD) [25–27]. $\gamma\gamma$+2 jets are also the main irreducible background for other physics analyses with $\gamma\gamma$ and jets in the final state at the LHC, such as Higgs produced in vector boson fusion. For the production of $\gamma\gamma$+2 jets, a sizeable contribution from DPS with $\gamma\gamma$ produced in one scattering while the second scattering yielding two jets can be expected. This DPS process was discussed in [28], based on leading order consideration for p$\bar{\text{p}}$ colli-

Received 20 April 2015, Revised 20 July 2015

∗ Supported by National Natural Science Foundation of China (11061140514, 11505208), China Ministry of Science and Technology (2013CB838700) and CAS Center for Excellence in Particle Physics (CCEPP)

1) E-mail: taojq@mail.ihep.ac.cn

sions at the Tevatron ($\sqrt{s}$=1.8 TeV). This is the first time for the calculation of its production in pp collisions at the LHC and the estimated sufficient event rates for its measurement with the incoming 13 TeV data and future 14 TeV data at the LHC.

The structure of this paper is organized as follows. In Section 2, a generic formula for the DPS cross section as the product of the SPS cross sections and its parameter are briefly introduced. The details of the cross section of $\gamma\gamma$+2 jets calculation and the cross section of different SPS processes estimated from higher order theoretical predictions are described in Section 3. The results including the cross section of $\gamma\gamma$+2 jets with $\sqrt{s}$=13 TeV and 14 TeV at LHC and the expected event rates, with typical selections, are summarized in Section 4. The summary and outlook are given in Section 5.

2 Generic formula for DPS

For a composite system (A+B) in hadronic collisions, its production cross section from DPS, $\sigma^{\rm DPS}_{\rm pp\to AB}$, can be written model-independently as the product of the cross sections of A and B originated from single parton scattering, $\sigma^{\rm SPS}_{\rm pp\to A}$ and $\sigma^{\rm SPS}_{\rm pp\to B}$, normalized by an effective cross section $\sigma_{\rm eff}$ [29]

$$\sigma^{\rm DPS}_{\rm pp\to AB}=\frac{m}{2}\frac{\sigma^{\rm SPS}_{\rm pp\to A}\times\sigma^{\rm SPS}_{\rm pp\to B}}{\sigma_{\rm eff}}, \quad (1)$$

where m is a symmetry factor accounting for distinguishable (m=2) and indistinguishable (m=1) final-states.

The effective cross section $\sigma_{\rm eff}$ is a measure of the transverse distribution of partons inside the colliding hadrons and their overlap in a collision. It is independent of the process and of the phase-space under consideration. A number of measurements of $\sigma_{\rm eff}$ have been performed in pp and p$\bar{\rm p}$ collisions at $\sqrt{s}$=63 GeV [6], 630 GeV [7], 1.8 TeV [8, 9, 30], 1.96 TeV [10] and also 7 TeV at LHC [3, 4]. The measured values range from 5 mb at the lowest energy to about 20 mb from CMS at 7 TeV. Figure 1 shows a comparison of the effective cross section $\sigma_{\rm eff}$ measured by different experiments using different processes at various centre-of-mass energies.

The measured values of $\sigma_{\rm eff}$ from TeV experiments at Tevetron (CDF and D0) and LHC (ATLAS and CMS) are consistent with each other within their uncertainties. In the following calculations, a numerical value $\sigma_{\rm eff}\approx$15 mb was used to estimate the production cross section of $\gamma\gamma$+2jets from DPS with $\sqrt{s}$=13 TeV and 14 TeV at LHC. A number 5 mb was assigned as its uncertainty to estimate its effects on the final results. The uncertainty in $\sigma_{\rm eff}$ is the dominant uncertainty for the calculation of the production cross section of $\gamma\gamma$+2 jets from DPS in the following sections.

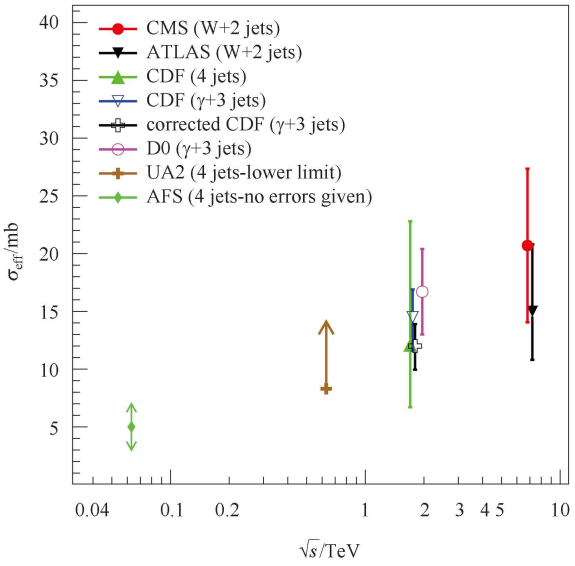

Fig. 1. (color online) $\sigma_{\rm eff}$ measured by different experiments using different processes [3, 4, 6–10, 30]. The "corrected CDF" data point indicate the $\sigma_{\rm eff}$ value corrected for the exclusive event selection [30].

3 $\sigma^{\rm DPS}_{\rm pp\to\gamma\gamma+2jets}$ calculation

According to the description in Section 2, the production cross section of $\gamma\gamma$+2 jets from DPS in pp collisions can be written as

$$\sigma^{\rm DPS}_{\rm pp\to\gamma\gamma+2jets} = \frac{\sigma^{\rm SPS}_{\rm pp\to\gamma\gamma}\times\sigma^{\rm SPS}_{\rm pp\to 2jets}}{\sigma_{\rm eff}} + \frac{1}{2}\frac{\sigma^{\rm SPS}_{\rm pp\to\gamma+jet}\times\sigma^{\rm SPS}_{\rm pp\to\gamma+jet}}{\sigma_{\rm eff}}. \quad (2)$$

$\gamma\gamma$ production has been calculated at next-to-leading-order (NLO) some time ago [31], supplemented also by gluon-initiated subprocesses beyond the leading order [32] and soft gluon resummation [33, 34]. Recently, next-to-next-to-leading-order (NNLO) corrections to direct diphoton production have also become available [35]. The measurements from LHC [25–27] show that the NNLO can give much better agreement with measured data than the lower order predictions. For the integrated cross section, the predicted values by NNLO are almost exactly the same [27] or consistent within the uncertainties [25, 26] with the measured ones. So the production cross sections of $\gamma\gamma$ final-state from SPS, $\sigma^{\rm SPS}_{\rm pp\to\gamma\gamma}$, with different $\sqrt{s}$ will be obtained from the NNLO calculation with the package 2γNNLO.

For the dijet cross section, the measured data at LHC [36, 37] can be well described by NLO perturbative QCD (pQCD) calculations from the NLOJet++ program [38], corrected to account for non-perturbative and electroweak effects. From [36], the non-perturbative cor-

rection is within 3% for jets reconstructed with the anti-k_t clustering algorithm [39] and distance parameter or cone size R=0.4. The corrections for the electroweak effect can be negligible if the dijet mass is less than about 1 TeV. In this analysis, the NLO calculations of $\sigma^{\rm SPS}_{\rm pp\to 2jets}$ are performed using NLOJet++ (version 4.1.3) within the framework of the fastNLO package (version 2.3.1) [40].

The NLO pQCD prediction from the program JETPHOX (version 1.3.1) [41] is used for the calculation of γ+jet cross sections from SPS in this paper. This program includes a full NLO QCD calculation of both the direct-photon and fragmentation contributions to the cross section. The number of flavours was set to five. Compared with the measurements of γ+jet cross sections at the LHC, the predictions from JETPHOX multiplied by a factor close to unity for the corrections of hadronisation and underlying-event effects give a good description of the transverse momenta of photon ($E^{\gamma}_{\rm T}$) and jet ($p^{\rm jet}_{\rm T}$) measured cross sections [42, 43].

Different PDF sets are used for the calculations of these three SPS processes. MSTW2008NNLO [44] is used for $\sigma^{\rm SPS}_{\rm pp\to\gamma\gamma}$ calculations with 2γNNLO. CT10NLO [45] is used for both $\sigma^{\rm SPS}_{\rm pp\to 2jets}$ with NLOJet++ in fastNLO package and $\sigma^{\rm SPS}_{\rm pp\to\gamma+jet}$ with JETPHOX.

The calculations of $\sigma^{\rm SPS}_{\rm pp\to\gamma\gamma}$ are performed with the factorization and renormalization scales equal to the invariant mass of two photons, $\mu_{\rm F}=\mu_{\rm R}=m_{\gamma\gamma}$. The scale uncertainty and PDF uncertainty are also considered. A simplified and less computationally intensive estimate of the renormalization ($\mu_{\rm R}$) and factorization ($\mu_{\rm F}$) scale uncertainties are performed by varying these scales simultaneously by a factor of two up and down around $m_{\gamma\gamma}$, $\mu_{\rm F}=\mu_{\rm R}=2m_{\gamma\gamma}$ and $\mu_{\rm F}=\mu_{\rm R}=0.5m_{\gamma\gamma}$. Forty-one eigenvector sets of MSTW2008NNLO are used to build the PDF uncertainty envelope.

Calculations of $\sigma^{\rm SPS}_{\rm pp\to 2jets}$ are derived using NLOJet++ within the framework of the fastNLO package at a factorization and renormalization scale equal to the average transverse momentum ($p^{\rm ave}_{\rm T}$) of the two jets ($\mu_{\rm F}=\mu_{\rm R}=p^{\rm ave}_{\rm T}$). The uncertainty due to the choice of factorization and renormalization scales is estimated as the maximum deviation at the six points ($\mu_{\rm F}/\mu$, $\mu_{\rm R}/\mu$)=(0.5, 0.5), (2, 2), (1, 0.5), (1, 2), (0.5, 1), (2, 1) with $\mu=p^{\rm ave}_{\rm T}$. Fifty-two eigenvector sets of CT10NLO are used to build the PDF uncertainty envelope.

For NLO calculations of $\sigma^{\rm SPS}_{\rm pp\to\gamma+jet}$ using JETPHOX, the renormalization, factorization and fragmentation ($\mu_{\rm f}$) scales are chosen to be the photon's transverse momentum, $\mu_{\rm F}=\mu_{\rm R}=\mu_{\rm f}=E^{\gamma}_{\rm T}$. Scale uncertainties, with the same consideration as the $\sigma^{\rm SPS}_{\rm pp\to\gamma\gamma}$ calculations, are performed by varying these scales simultaneously by a factor of two up and down around $E^{\gamma}_{\rm T}$. As the calculations of $\sigma^{\rm SPS}_{\rm pp\to 2jets}$, 52 eigenvector sets of CT10NLO are used to build the PDF uncertainty envelope.

The above calculations were performed with the strong coupling constant at two-loop order with $\alpha_{\rm s}(m_{\rm Z})$= 0.118 in CT10NLO and 0.117 in MSTW2008NNLO. The uncertainty in $\alpha_{\rm s}(m_{\rm Z})$ was not considered in this study. The uncertainty from scales, pdf and $\alpha_{\rm s}(m_{\rm Z})$ is around 10%, 5% and 1% respectively [25–27, 36, 37, 42, 43]. Compared to the larger uncertainty in the $\sigma_{\rm eff}$, with a value of more than 30% used in this study as explained at the end of Section 2, the effect on the final results from the uncertainty in $\alpha_{\rm s}(m_{\rm Z})$ should be negligible.

4 Results of $\sigma^{\rm DPS}_{\rm pp\to\gamma\gamma+2jets}$ and expected event rates at LHC

In this paper, several sets of typical selections at LHC were used to calculate the production cross section of $\gamma\gamma$+2jets from DPS in pp collisions, $\sigma^{\rm DPS}_{\rm pp\to\gamma\gamma+2jets}$. Due to the high level trigger requirements for $\gamma\gamma$ events at LHC for the higher energy and higher luminosity collisions, five sets of requirements on the photon transverse momenta were considered, ($E^{\gamma_1}_{\rm T}$, $E^{\gamma_2}_{\rm T}$) >(30, 20) GeV, (30, 30) GeV, (40, 20) GeV, (40, 30) GeV and (40, 40) GeV, with γ_1 representing the maximum $E_{\rm T}$ photon and γ_2 the minimum $E_{\rm T}$ photon of the two photons. For the single photon requirement in the γ+jet, three cases with $E^{\gamma}_{\rm T}>$ (20, 30, 40) GeV were considered. The photon should also be constrained in the pseudorapidity region $|\eta|<$2.5. An isolation requirement is applied on the photon to fulfill the isolation requirement from experimental measurements [25–27, 42, 43]. The standard isolation, the $E_{\rm T}$ sum of partons in a cone of size ΔR=0.4 around the photon required to less than 5 GeV, is applied in JETPHOX for the calculation of $\sigma^{\rm SPS}_{\rm pp\to\gamma+jet}$. For 2$\gamma$NNLO, the smooth Frixione isolation [46] on the photons is applied

$$E^{\rm iso}_{\rm T}(\Delta R)<\epsilon\left(\frac{1-\cos(\Delta R)}{1-\cos(\Delta R_0)}\right)^n, \qquad (3)$$

where $E^{\rm iso}_{\rm T}(\Delta R)$ is the $E_{\rm T}$ sum of partons in a cone of size ΔR, ΔR_0=0.4, ϵ=5 GeV, and n=0.1. This criterion is found to have the same efficiency as the standard isolation used for the other generators within a few percent [25, 26]. Additionally, the angular separation between two photons is required to be at least larger than 0.4 ($\Delta R_{\gamma\gamma}>$0.4) to ensure one photon will not enter the isolation cone of the other photon, which is similar to the requirement applied in the data analyses at the LHC experiments ATLAS and CMS [25–27].

In this study, jets are reconstructed with the anti-k_t clustering algorithm and cone size R=0.5. Jets are in the acceptance region with $|\eta^{\rm jet}|<$4.5. Two tries on jet $p^{\rm jet}_{\rm T}$ were performed, $p^{\rm jet}_{\rm T}>$ 20 or 25 GeV. For the dijet events, the two jets should be separated by requiring

their angular distance $\Delta R_{\rm jj}$ to be greater than 1.0 to avoid the overlapping of the two jet cones. For the γ+jet production, the angular distance between γ and jet should be greater than 0.5 ($\Delta R_{\gamma \rm j} > 0.5$) to ensure that the partons belonging to the jet will not enter to the isolation cone of the γ.

Figure 2 shows the cross sections of $\sigma^{\rm SPS}_{\rm pp\to\gamma\gamma}$ computed from the 2γNNLO at $\sqrt{s}$=13 TeV and 14 TeV with scales and pdf uncertainties considered, for different sets of $E_{\rm T}$ requirements on diphotons. The scale uncertainty is around 10% and the pdf uncertainty is about 4%. The selection sets on the x-axis are the five sets of requirements on ($E^{\gamma_1}_{\rm T}$, $E^{\gamma_2}_{\rm T}$), number 1 for ($E^{\gamma_1}_{\rm T}$, $E^{\gamma_2}_{\rm T}$)>(30, 20) GeV, 2 for ($E^{\gamma_1}_{\rm T}$, $E^{\gamma_2}_{\rm T}$)>(30, 30) GeV, 3 for ($E^{\gamma_1}_{\rm T}$, $E^{\gamma_2}_{\rm T}$)>(40, 20) GeV, 4 for ($E^{\gamma_1}_{\rm T}$, $E^{\gamma_2}_{\rm T}$)>(40, 30) GeV and 5 for ($E^{\gamma_1}_{\rm T}$, $E^{\gamma_2}_{\rm T}$)>(40, 40) GeV. The detailed values can also be found in Table 1. For the central values, the cross section with $\sqrt{s}$=14 TeV is about 9% higher than that with $\sqrt{s}$=13 TeV with the same selection requirements, which is within the scale and pdf uncertainties.

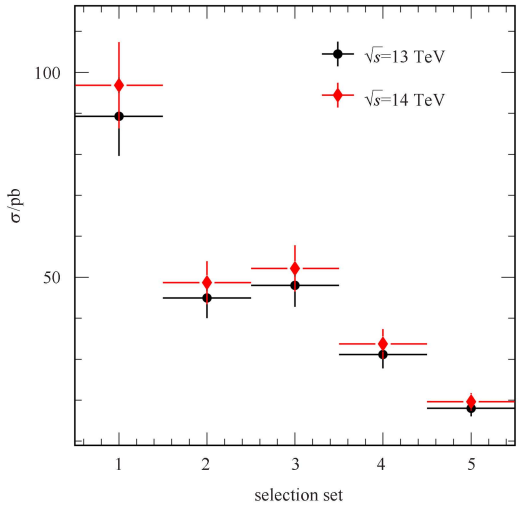

Fig. 2. (color online) Predicted cross sections of $\gamma\gamma$ by 2γ NNLO at $\sqrt{s}$=13 TeV and 14 TeV with selection set 1 for ($E^{\gamma_1}_{\rm T}$, $E^{\gamma_2}_{\rm T}$)>(30, 20) GeV, 2 for ($E^{\gamma_1}_{\rm T}$, $E^{\gamma_2}_{\rm T}$)>(30, 30) GeV, 3 for ($E^{\gamma_1}_{\rm T}$, $E^{\gamma_2}_{\rm T}$)>(40, 20) GeV, 4 for ($E^{\gamma_1}_{\rm T}$, $E^{\gamma_2}_{\rm T}$)>(40, 30) GeV and 5 for ($E^{\gamma_1}_{\rm T}$, $E^{\gamma_2}_{\rm T}$)>(40, 40) GeV. Scale and pdf uncertainties are included.

Figure 3 shows the differential cross sections, as a function of the $p_{\rm T}$ of leading jet with both jet $p^{\rm jet}_{\rm T}$ > 20 GeV and $|\eta|$<4.5, of $\sigma^{\rm SPS}_{\rm pp\to 2jets}$ computed from NLOJet++ within the framework of the fastNLO package at $\sqrt{s}$=13 TeV and 14 TeV with scales and pdf uncertainties plotted in the same figure. The bottom two plots show the relative uncertainties including the scale uncertainty and scale⊕pdf uncertainty combined in quadrature. The contribution of pdf uncertainty is tiny. The integrated cross sections are $117.6^{+4.8}_{-7.0}$(scale)$^{+1.0}_{-1.3}$(pdf) (μb) and $122.3^{+4.6}_{-5.1}$(scale) $^{+1.1}_{-1.4}$(pdf) (μb) for $\sqrt{s}$ = 13 TeV and 14 TeV with both jet $p^{\rm jet}_{\rm T}$ > 20 GeV and $|\eta^{\rm jet}|$ < 4.5, $52.2^{+1.6}_{-2.4}$(scale)$^{+0.4}_{-0.5}$(pdf) (μb) and $56.2^{+1.8}_{-2.3}$(scale) $^{+0.5}_{-0.6}$(pdf) (μb) for $\sqrt{s}$=13 TeV and 14 TeV with both jet $p^{\rm jet}_{\rm T}$> 25 GeV and $|\eta^{\rm jet}|$< 4.5. When $p_{\rm T}$ requirements on both jets increase 5 GeV from 20 GeV to 25 GeV, the cross sections are reduced almost by a factor of 2.

Table 1. Cross sections in units of pb of $\gamma\gamma$ predicted by 2γ NNLO at $\sqrt{s}$=13 TeV and 14 TeV. The uncertainties include the scale and pdf uncertainties.

($E^{\gamma_1}_{\rm T}$, $E^{\gamma_2}_{\rm T}$)>	$\sqrt{s}$=13 TeV	$\sqrt{s}$=14 TeV
(30, 20) GeV	89.3±9.7	96.9±10.5
(30, 30) GeV	44.9±4.9	48.7±5.3
(40, 20) GeV	48.0±5.2	52.1±5.7
(40, 30) GeV	31.2±3.4	33.7±3.7
(40, 40) GeV	18.0±2.0	19.6±2.1

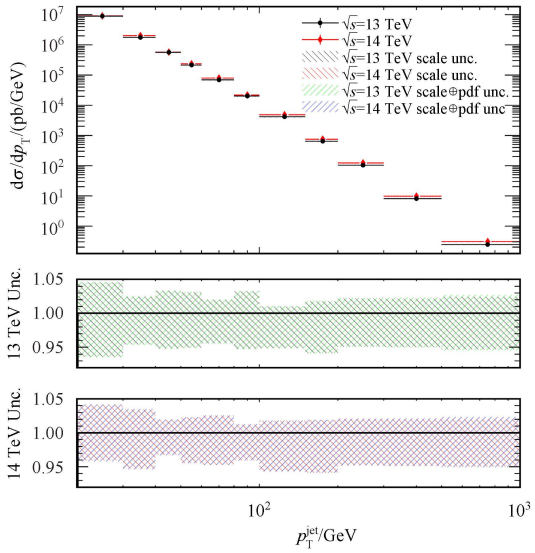

Fig. 3. (color online) Differential cross sections of jet+jet computed with NLOJet++ within the framework of the fastNLO package, after the requirements on both jets with $p^{\rm jet}_{\rm T}$ > 20 GeV and $|\eta^{\rm jet}|$ <4.5. The solid black circles are the results for $\sqrt{s}$=13 TeV and the red diamonds are for $\sqrt{s}$=14 TeV. The bottom two plots show the relative uncertainties including the scale uncertainty and scale⊕pdf uncertainty, with $\sqrt{s}$=13 TeV in the middle plot and $\sqrt{s}$=14 TeV in the bottom plot.

Combining the photon $E^{\gamma}_{\rm T}$ requirements for the $\gamma\gamma$ productions and the jet $p^{\rm jet}_{\rm T}$ requirements for the jet+jet productions, the cross section of $\sigma^{\rm SPS}_{\rm pp\to\gamma+jet}$ with six sets of selections on the transverse momenta of photons and jets with ($E^{\gamma}_{\rm T}$, $p^{\rm jet}_{\rm T}$)>(20, 20) GeV, (30, 20) GeV, (40, 20) GeV, (20, 25) GeV, (30, 25) GeV and (40, 25) GeV were calculated. Figure 4 shows the differential cross sections of $\sigma^{\rm SPS}_{\rm pp\to\gamma+jet}$ as a function of photon $E^{\gamma}_{\rm T}$ with ($E^{\gamma}_{\rm T}$,

$p_{\rm T}^{\rm jet}$)>(40, 20) GeV, $|\eta^{\gamma}|$<2.5, $|\eta^{\rm jet}|$< 4.5 and separation $\Delta R_{\gamma {\rm j}}$>0.5, computed from JETPHOX with $\sqrt{s}$=14 TeV. The contributions from the direct photon production and photon from fragmentation are shown in the same plot. The scales and pdf uncertainties are also plotted in the same figure. The integrated cross sections are listed in Table 2 for different sets of selections and collision energies. The scale and pdf uncertainties are also listed in this table, with about 10% uncertainty from scales and around 4% from pdf.

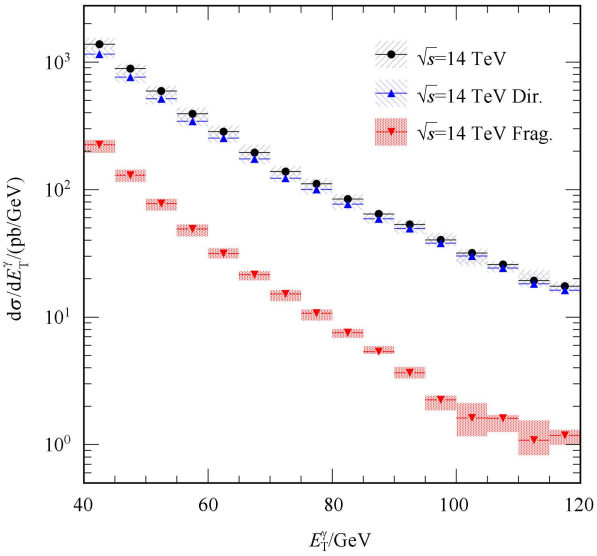

Fig. 4. (color online) Differential cross sections of γ+jet as a function of the photon $E_{\rm T}^{\gamma}$, computed with JETPHOX and the selections ($E_{\rm T}^{\gamma}$, $p_{\rm T}^{\rm jet}$)>(40, 20) GeV, $|\eta^{\gamma}| < 2.5$, $|\eta^{\rm jet}| < 4.5$ and separation $\Delta R_{\gamma {\rm j}} > 0.5$ at $\sqrt{s}$=14 TeV. The solid circles are the total contributions while the blue triangles represent the direct contribution and the red triangles are the contributions of photons from fragmentation. Scales and pdf uncertainties are also shown in this plot.

Table 2. Cross sections in units of 10^3 pb of γ+jet predicted by JETPHOX at $\sqrt{s}$ = 13 TeV and 14 TeV. The total uncertainties including scale uncertainty and pdf uncertainty are also listed in this table.

($E_{\rm T}^{\gamma}$, $p_{\rm T}^{\rm jet}$)>	$\sqrt{s}$=13 TeV	$\sqrt{s}$=14 TeV
(20, 20) GeV	$90.1^{+11.0}_{-9.6}$	$97.2^{+13.3}_{-11.6}$
(30, 20) GeV	$48.7^{+5.2}_{-4.6}$	$52.7^{+5.7}_{-5.0}$
(40, 20) GeV	$20.2^{+2.2}_{-1.8}$	$22.0^{+2.5}_{-2.1}$
(20, 25) GeV	$85.0^{+9.8}_{-8.7}$	$91.7^{+10.9}_{-9.1}$
(30, 25) GeV	$41.5^{+4.4}_{-3.9}$	$45.0^{+4.7}_{-4.4}$
(40, 25) GeV	$19.7^{+2.0}_{-1.8}$	$21.4^{+2.4}_{-1.9}$

According to Eq. (2) and the above cross sections of the SPS processes, the cross sections for the production of pairs of photons plus two additional jets produced from double parton scattering (DPS) in high-energy proton-proton collisions at the LHC are calculated for the first time. The results are summarized in Table 3. Two jets in the same pp $\rightarrow \gamma\gamma$+2jets event from DPS have the same $p_{\rm T}$ cut thresholds, both $p_{\rm T}^{\rm jet}$ > 20 GeV or 25 GeV simultaneously. The calculated cross section can be around 0.1 pb to ~1 pb with the selections considered in this paper. The uncertainty on the cross section is around 50%, with the dominant contribution from the uncertainty of $\sigma_{\rm eff}$.

Table 3. Cross sections in units of pb of $\sigma^{\rm DPS}_{{\rm pp}\rightarrow\gamma\gamma+2{\rm jets}}$ calculated for $\sqrt{s}$=13 TeV and 14 TeV with the selections described in the paper. The total uncertainties including scale uncertainty, pdf uncertainty and also the $\sigma_{\rm eff}$ uncertainty are also listed in this table.

($E_{\rm T}^{\gamma_1}$, $E_{\rm T}^{\gamma_2}$, both $p_{\rm T}^{\rm jet}$)>	$\sqrt{s}$=13 TeV	$\sqrt{s}$=14 TeV
(30, 20, 20) GeV	$0.846^{+0.423}_{-0.432}$	$0.960^{+0.481}_{-0.479}$
(30, 20, 25) GeV	$0.428^{+0.213}_{-0.215}$	$0.500^{+0.250}_{-0.250}$
(30, 30, 20) GeV	$0.431^{+0.215}_{-0.219}$	$0.489^{+0.243}_{-0.242}$
(30, 30, 25) GeV	$0.428^{+0.213}_{-0.215}$	$0.250^{+0.124}_{-0.124}$
(40, 20, 20) GeV	$0.437^{+0.218}_{-0.222}$	$0.496^{+0.247}_{-0.247}$
(40, 20, 25) GeV	$0.223^{+0.113}_{-0.111}$	$0.261^{+0.130}_{-0.129}$
(40, 30, 20) GeV	$0.277^{+0.137}_{-0.141}$	$0.313^{+0.155}_{-0.155}$
(40, 30, 25) GeV	$0.136^{+0.068}_{-0.067}$	$0.159^{+0.078}_{-0.078}$
(40, 40, 20) GeV	$0.154^{+0.076}_{-0.079}$	$0.176^{+0.086}_{-0.087}$
(40, 40, 25) GeV	$0.076^{+0.038}_{-0.037}$	$0.089^{+0.044}_{-0.043}$

With an integrated luminosity of 100 fb^{-1} at $\sqrt{s}$=13 TeV accumulated in the following years, about 85k pp $\rightarrow \gamma\gamma$+2jets events from DPS can be obtained with the loosest selections, diphoton ($E_{\rm T}^{\gamma_1}$, $E_{\rm T}^{\gamma_2}$)>(30, 20) GeV and both jets $p_{\rm T}^{\rm jet}$>20 GeV. These events can be triggered by the diphoton paths proposed at the LHC for $\sqrt{s}$=13 TeV. When the integrated luminosity increases at $\sqrt{s}$=14 TeV, tighter $E_{\rm T}$ thresholds on diphoton for the trigger will be used. With the tighter selections, diphoton ($E_{\rm T}^{\gamma_1}$, $E_{\rm T}^{\gamma_2}$)>(40, 30) GeV and both jets $p_{\rm T}^{\rm jet}$>20 GeV, about 940k pp$\rightarrow\gamma\gamma$+2jets events from DPS can be obtained with an integrated luminosity of 3000 fb^{-1}. Even with the tightest selections studied in this paper, diphoton ($E_{\rm T}^{\gamma_1}$, $E_{\rm T}^{\gamma_2}$)>(40, 40) GeV and both jets $p_{\rm T}^{\rm jet}$>25 GeV, we can also get about 260 k pp$\rightarrow\gamma\gamma$+2jets events from DPS with 3000 fb^{-1} as designed by LHC.

5 Summary and outlook

In this paper, the cross sections for the production of pairs of photons plus two additional jets produced from double parton scattering in high-energy proton-proton collisions at the LHC with $\sqrt{s}$=13 TeV and 14 TeV (LHC Run2) are calculated for the first time. With the generic formula, the cross sections have been computed based on

the theoretical perturbative QCD predictions for the productions of $\gamma\gamma$ at next-to-next-to-leading-order, jet+jet and γ+jet at next-to-leading-order, with their corresponding single-scattering cross sections. From the LHC measurements with the collision data obtained in the years 2011 and 2012 (LHC Run1), these theoretical predictions for these three SPS processes give the best agreements with the measured data. With the typical acceptance and selections used at LHC, the cross sections $\sigma^{\rm DPS}_{\rm pp\to\gamma\gamma+2jets}$ can be estimated to be around 0.1 pb to 1 pb with the collision energy $\sqrt{s}$=13 TeV or 14 TeV. The expected event rates for $\gamma\gamma$+2jets from DPS, with some sets of selections, are given for proton-proton collisions with the collision energy $\sqrt{s}$=13 TeV and an integrated luminosity of 100 fb^{-1} planned for the following two years, and also $\sqrt{s}$=14 TeV with 3000 fb^{-1} of integrated luminosity as the LHC design. The uncertainties in the cross section and event rates are mainly dominated by the $\sigma_{\rm eff}$ uncertainty. The scale and pdf uncertainties for the productions of these three SPS processes are also considered.

With the incoming LHC Run2 data, there are enough pp $\to\gamma\gamma$+2jets events from DPS for investigations. It needs further studies on the variables, such as the angles between the two photons and two jets, to be chosen for the discrimination of pp $\to\gamma\gamma$+2jets events from DPS and pp $\to\gamma\gamma$+2jets events from SPS when performing the data analysis. Also the effect of contributions from the DPS to the whole pp$\to\gamma\gamma$+2jets event rate on the distributions of some typical variables need detailed investigations in the LHC Run2 data analysis.

The authors would like to thank Dr. Hua-Sheng Shao from CERN for helpful discussions and Leandro Cieri for his help with the NNLO matrix element generator 2γNNLO which is not public yet.

References

1 Landshoff P V, Polkinghorne J C. Phys. Rev. D, 1978, **18**: 3344
2 Lansberg J P, Shao H S. arXiv:hepph/1410.8822
3 Aad G et al (ATLAS collaboration). New J. Phys., 2013, **15**: 033038
4 Chatrchyan S et al (CMS collaboration). J. High Energy Phys., 2014, **1403**: 032
5 Aad G et al (ATLAS collaboration). J. High Energy Phys., 2014, **1405**: 068
6 Alitti J et al (UA2 collaboration). Phys. Lett. B, 1991, **268**: 145
7 Akesson T et al (AFS collaboration). Z. Phys. C, 1987, **34**: 163
8 Abe F et al (CDF collaboration). Phys. Lett. D, 1993, **47**: 4857
9 Abe F et al (CDF collaboration). Phys. Lett. D, 1997, **56**: 3811
10 Aaltonen T et al (CDF collaboration). Phys. Lett. D, 2010, **81**: 052012
11 Diehl M, Ostermeier D, Schafer A. J. High Energy Phys., 2012, **03**: 089
12 Calucci G, Treleani D. Phys. Rev. D, 2011, **83**: 016012
13 Fabbro A D, Treleani D. Phys. Rev. D, 2000, **61**: 077502
14 Hussein M. Nucl. Phys. Proc. Suppl., 2007, **174**: 55
15 Bandurin D, Golovanov G, Skachkov N. J. High Energy Phys., 2011, **04**: 054
16 Mekhfi M. Phys. Rev. D, 1985, **32**: 2371
17 Ametller L, Paver N, Treleani D. Phys. Lett. B, 1986, **169**: 289
18 Gaunt J R, Kom C H, Kulesza A, Stirling W J. Eur. Phys. J. C, 2010, **69**: 53
19 Chatrchyan S et al (CMS collaboration). Phys. Lett. B, 2012, **716**: 30
20 Aad G et al (ATLAS collaboration). Phys. Lett. B, 2012, **716**: 1
21 Aad G et al (ATLAS collaboration). Phys. Lett. B, 2012, **718**: 411
22 Aad G et al (ATLAS collaboration). New J. Phys., 2013, **15**: 043007
23 Chatrchyan S et al (CMS collaboration). Phys. Lett. B, 2013, **719**: 42
24 Chatrchyan S et al (CMS collaboration). J. High Energy Phys., 2013, **03**: 111
25 Chatrchyan S et al (CMS collaboration). Eur. Phys. J. C, 2014, **74**: 3129
26 TAO J Q. Nucl. Part. Phys. Proc., 2015, **258-259**: 7–10
27 Aad G et al (ATLAS collaboration). Phys. Rev. D, 2012, **85**: 012003
28 Drees M, HAN T. Phys. Rev. Lett., 1996, **77**: 4142–4145
29 Enterria D, Snigirev A M. Nucl. Phys. A, 2014, **931**: 303–308
30 Bahr M, Myska M, Seymour M H, Siodmok A. J. High Energy Phys., 2013, **03**: 129
31 Binoth T, Guillet J, Pilon E, Werlen M. Eur. Phys. J. C, 2000, **16**: 311
32 Bern Z, Dixon L J, Schmidt C. Phys. Rev. D, 2002, **66**: 074018
33 Balazs C, Nadolsky P M, Schmidt C, YUAN C P. Phys. Lett. B, 2000, **489**: 157
34 Balazs C, Berger E L, Nadolsky P M, Yuan C P. Phys. Lett. B, 2006, **637**: 235
35 Catani S, Cieri L, Florian D, Ferrera G, Grazzini M. Phys. Rev. Lett., 2012, **108**: 072001
36 Aad G et al (ATLAS collaboration). J. High Energy Phys., 2014, **05**: 059
37 Chatrchyan S et al (CMS collaboration). Phys. Lett. B, 2011, **700**: 187; Chatrchyan S et al (CMS collaboration). Eur. Phys. J. C, 2013, **73**: 2604; Chatrchyan S et al (CMS collaboration). Phys. Rev. D, 2013, **87**: 112002; Chatrchyan S et al (CMS collaboration). CMS-PAS-SMP-**14-002** 2014
38 Nagy Z. Phys. Rev. D, 2003, **68**: 094002
39 Cacciari M, Salam G P, Soyez G. J. High Energy Phys., 2008, **04**: 063
40 Kluge T, Rabbertz K, Wobisch M. arXiv:hep-ph/0609285v2
41 Catani S, Fontannaz M, Guillet J P, Pilon E. J. High Energy Phys., 2002, **05**: 028
42 Aad G et al (ATLAS collaboration). Nucl. Phys. B, 2013, **875**: 483–535
43 Chatrchyan S et al (CMS collaboration). Phys. Rev. Lett., 2011, **106**: 082001
44 Martin A D, Stirling W J, Thorne R S, Watt G. Eur. Phys. J. C, 2009, **63**: 189–285
45 LAI H L et al. Phys. Rev. D, 2010, **82**: 074024
46 Frixione S. Phys. Lett. B, 1998, **429**: 369